Article:
Lesnic, D. and Alosaimi, M. (2024) Retrieving the time-dependent blood perfusion coefficient in the thermal-wave model of bio-heat transfer. Engineering Computations, 41 (7). pp. 1824-1838. ISSN: 0264-4401

https://doi.org/10.1108/EC-01-2024-0013

Retrieving the time-dependent blood perfusion coefficient in the thermal-wave model of bio-heat transfer

Abstract. This paper aims to identify the time-dependent blood perfusion coefficient and the temperature in the thermal-wave model of bio-heat transfer from non-intrusive boundary temperature measurements that may be taken with an infrared scanner. The uniqueness of solution to this inverse coefficient problem is established. To find the solution, the nonlinear and ill-posed problem is recast as a nonlinear least-squares minimization with simple bounds on the unknown coefficient, and the Tikhonov regularization is employed to ensure stability. The Crank–Nicolson finite-difference scheme is employed to solve the direct problem. To solve the nonlinear least-squares minimization problem, we utilize the built-in subroutine *lsqnonlin* from the MATLAB optimization toolbox. Numerical results for a benchmark test example are presented and thoroughly discussed, shedding light on the performance and effectiveness of the proposed methodology.

Keywords: Inverse problem; bio-heat transfer; blood perfusion coefficient; Tikhonov regularization; thermal-wave model

1. Introduction

The transfer of heat in biological tissues is influenced by mechanisms such as conduction, blood circulation, blood-tissue convection and heat production from metabolic processes [14, 19], and its understanding plays a fundamental role in designing appropriate thermal therapies for anomaly detection and treatment [4]. Furthermore, the properties of the tissue and blood are usually not known precisely and have to be determined using inverse analysis [1, 2]. Based on this brief motivation, the novelty of the study consists mainly in the inverse mathematical modelling described in section 1 and analyzed mathematically in terms of uniqueness of solution in section 2, whilst sections 3 and 4 apply existing techniques to the newly-formulated direct and inverse problems. Section 5 discusses the numerically-obtained results and section 6 concludes the findings of the paper.

The equation governing the temperature T [°C] of the tissue is given by [9],

$$\rho_{\mathrm{t}} c_{\mathrm{t}} \frac{\partial T}{\partial \bar{t}} = -\nabla \cdot \mathbf{q} + \rho_b c_b w_b (T_b - T) + Q_m + Q_e, \tag{1}$$

where $\mathbf{q}$ is the thermal flux vector [W/m^2], ρ_{t} and c_{t} denote the density [kg/m^3] and specific heat [J/(kg °C)] of the tissue, respectively, ρ_b, c_b and w_b denote the density [kg/m^3], specific heat [J/(kg °C)] and perfusion rate [s^{-1}] of the blood, respectively, T_b denotes the (arterial) blood temperature [°C], Q_m and Q_e represent the production of heat resulting from metabolic processes and external heating [W/m^3], respectively, and $\bar{t}$ stands for the time [s]. The application of Fourier's law

$$\mathbf{q} = -\kappa \nabla T, \tag{2}$$

where κ represents the thermal conductivity [W/(m °C)] of the tissue, transforms equation

(1) into the well-known Pennes parabolic bio-heat transfer equation [17],

$$\rho_{\mathrm{t}} c_{\mathrm{t}} \frac{\partial T}{\partial \bar{t}} = \nabla \cdot (\kappa \nabla T) + \rho_b c_b w_b (T_b - T) + Q_m + Q_e. \tag{3}$$

The Pennes' equation (3) has demonstrated sufficient accuracy in approximating a broad array of physical phenomena. These include the forecasting of temperature changes during hyperthermia in cancer treatment [20], evaluating the thermal impacts of radiation from cellular phones [22], and guiding thermal therapies for removing diseased tissues [13], among others applications. The underlying parabolic PDE (3) implies that (as it is based on Fourier's law (2)) any thermal alteration within the medium affects all locations instantaneously, implying an infinite speed of thermal propagation. Nevertheless, when modelling heat transfer in biological organisms, there arises a significant relaxation time τ (typically ranging from 15 to 30 seconds) necessary for thermal waves to accumulate and propagate, [16]. This indicates that thermal waves propagate at a finite velocity. Cattaneo and Vernotte introduced a modification to Fourier's law (2) to incorporate this realistic physical feature. This modified equation, often referred to as the Maxwell-Cattaneo flux law, is expressed as:

$$\left(1 + \tau \frac{\partial}{\partial \bar{t}}\right) \mathbf{q} = -\kappa \nabla T. \tag{4}$$

Here, $\tau = \alpha / \mathrm{c}^2$, where $\alpha = \kappa / (\rho_{\mathrm{t}} c_{\mathrm{t}})$ represents the thermal diffusivity of the tissue $[\mathrm{m}^2/\mathrm{s}]$, and c denotes the velocity of thermal waves $[\mathrm{m}/\mathrm{s}]$. This equation models that heat transfer mechanism in biological tissues arises not solely through diffusion but also through a wave-like phenomenon termed "second-sound", [7]. Assuming that the heat capacities of the tissue $C_{\mathrm{t}} = \rho_{\mathrm{t}} c_{\mathrm{t}}$ and blood $C_b = \rho_b c_b$ in $[\mathrm{J}/(\mathrm{m}^3\ ^\circ\mathrm{C})]$ are constant, that the arterial blood temperature T_b and (for simplicity) the thermal conductivity κ are constant, and that the blood perfusion rate $w_b = w_b(\bar{t})$ is time-dependent, introducing (4) into (1) results in:

$$\begin{aligned} C_{\mathrm{t}} \tau \frac{\partial^2 T}{\partial \bar{t}^2} + \left(C_{\mathrm{t}} + \tau C_b w_b(\bar{t})\right) \frac{\partial T}{\partial \bar{t}} = \kappa \nabla^2 T + C_b \left(w_b(\bar{t}) + \tau \frac{dw_b}{d\bar{t}}(\bar{t})\right)(T_b - T) \\ + Q_m + Q_e + \tau \frac{\partial}{\partial \bar{t}}(Q_m + Q_e). \end{aligned} \tag{5}$$

We consider the hyperbolic PDE (5) in the solution domain $\tilde{\Omega} \times (0, \bar{t}_{\mathrm{f}})$, where $\tilde{\Omega}$ is the bounded tissue domain and $\bar{t}_{\mathrm{f}} > 0$ is a final time of interest, subject to the initial conditions

$$T(\overline{\mathbf{x}}, 0) = \overline{\eta}(\overline{\mathbf{x}}), \quad \frac{\partial T}{\partial \bar{t}}(\overline{\mathbf{x}}, 0) = 0, \quad \overline{\mathbf{x}} \in \tilde{\Omega}, \tag{6}$$

where $\overline{\eta}$ is a prescribed function, and the adiabatic boundary condition

$$\frac{\partial T}{\partial n} = 0 \quad \text{on } \partial\tilde{\Omega} \times (0, \bar{t}_{\mathrm{f}}), \tag{7}$$

where $\mathbf{n}$ denotes the outward unit normal to the boundary $\partial\tilde{\Omega}$. In the inverse problem, when the blood perfusion rate $w_b = w_b(\bar{t})$ is unknown, as an additional measurement to compensate for this missing information, we consider (non-intrusively) measuring the boundary

temperature

$$T = \overline{h} \quad \text{on } \tilde{\Gamma} \times (0, \bar{t}_{\rm f}), \tag{8}$$

on an accessible subportion $\tilde{\Gamma} \subset \partial\tilde{\Omega}$, with an infrared scanner. Alternatively, one could measure the energy/mass of the biothermal system given by

$$\int_{\tilde{\Omega}} \chi(\overline{\mathbf{x}}) T(\overline{\mathbf{x}}, \bar{t}) d\overline{\mathbf{x}} = E(\bar{t}), \quad \bar{t} \in \big(0, \bar{t}_{\rm f}\big), \tag{9}$$

where χ is a prescribed function, [5, 6].

The related inverse problem concerning the identification of the space-dependent blood perfusion rate $w_b(\overline{\mathbf{x}})$ was recently investigated in [3, 10]. Relevant literature in the field of coefficient identification problems can be found in the books [11, 12, 15, 18], which include particular references to inverse problems for hyperbolic PDEs.

The inverse formulation (5)–(8) provides a suitable model for non-destructive testing via temperature measurements on an accessble portion $\tilde{\Gamma}$ of the full boundary $\partial\tilde{\Omega}$. Also, remark that the inverse problem of determining the time-dependent blood perfusion rate $w_b(\bar{t})$ from the boundary temperature measurement (8) is determined in one-dimension but it is over-determined in higher dimensions.

Before performing any analysis, the dimensional model (5)–(8) is non-dimensionalized, as described in the next subsection.

1.1 Non-dimensionalization

The thermal-wave model of bio-heat transfer (5)–(8) can be non-dimensionalized, as follows. Supposing a non-zero constant arterial blood temperature T_b, we propose the subsequent dimensionless variables:

$$\mathbf{x} = \sqrt{\frac{C_{\rm t}}{\kappa\tau}}\,\overline{\mathbf{x}}, \quad (t, t_{\rm f}) = \frac{1}{\tau}\big(\bar{t}, \bar{t}_{\rm f}\big), \quad z = \frac{T - T_b}{T_b}, \quad \eta = \frac{\overline{\eta} - T_b}{T_b},$$
$$h = \frac{\overline{h} - T_b}{T_b}, \quad F = \frac{\tau(Q_m + Q_e)}{T_b C_{\rm t}}, \quad k = \frac{\tau C_b w_b}{C_{\rm t}}. \tag{10}$$

Then, the dimensionless form of the thermal-wave model (5)–(8) (denoting $f = F + F_t$) can be written as

$$\frac{\partial^2 z}{\partial t^2}(\mathbf{x}, t) + \big(1 + k(t)\big)\frac{\partial z}{\partial t}(\mathbf{x}, t) = \nabla^2 z(\mathbf{x}, t) - \big(k(t) + k'(t)\big) z(\mathbf{x}, t) + f(\mathbf{x}, t),$$
$$(\mathbf{x}, t) \in \Omega \times (0, t_{\rm f}), \tag{11}$$

subject to the initial conditions

$$z(\mathbf{x}, 0) = \eta(\mathbf{x}), \quad \frac{\partial z}{\partial t}(\mathbf{x}, 0) = 0, \quad \mathbf{x} \in \Omega, \tag{12}$$

the adiabatic boundary condition

$$\frac{\partial z}{\partial n} = 0 \quad \text{on } \partial\Omega \times (0, t_{\rm f}), \tag{13}$$

and extra boundary temperature measurement

$$z = h \quad \text{on } \Gamma \times (0, t_{\mathrm{f}}), \tag{14}$$

where the normal derivative has kept the same notation, and Ω and Γ are the non-dimensional version of $\tilde{\Omega}$ and $\tilde{\Gamma}$, via the space dimensionalization in (10).

2. Analysis in one-space dimension

In one-dimension, let $\tilde{\Omega} = (0, \overline{L})$, where $\overline{L}$ in [m] is the physical dimension of a finite slab tissue. Denote also the non-dimensional length

$$L = \sqrt{\frac{C_{\mathrm{t}}}{\kappa\tau}}\, \overline{L}.$$

Then, the inverse problem (11)–(14) simplifies as:

$$\frac{\partial^2 z}{\partial t^2}(x,t) + \big(1 + k(t)\big)\frac{\partial z}{\partial t}(x,t) = \frac{\partial^2 z}{\partial x^2}(x,t) - \big(k(t) + k'(t)\big)z(x,t) + f(x,t), \quad (x,t) \in (0,L) \times (0,t_{\mathrm{f}}) =: Q, \tag{15}$$

$$z(x,0) = \eta(x), \quad \frac{\partial z}{\partial t}(x,0) = 0, \quad x \in (0,L), \tag{16}$$

$$\frac{\partial z}{\partial x}(0,t) = \frac{\partial z}{\partial x}(L,t) = 0, \quad t \in (0,t_{\mathrm{f}}), \tag{17}$$

$$z(0,t) = h(t), \quad t \in (0,t_{\mathrm{f}}), \tag{18}$$

where we took $\Gamma = \{x = 0\}$ as the accessible part of the boundary. The analogy of the problem (15)–(18) with the problem considered in [21] is given by

$$a(x,t) = 1 + k(t), \quad q(t) = k(t) + k'(t),$$

$$u_0(x) = \eta(x), \quad u_1(x) = 0, \quad \varphi_1(t) = \psi_1(t) = 0,$$

$$\varphi_0(t) = h(t), \quad D = (0,1) = (0,L).$$

The uniqueness of the solution $\big(z(x,t), k(t)\big)$ is established in the following theorem.

Theorem 1. *Assume that the input data $f \in H^3(Q)$, $\eta \in H^5(0,L)$ and $h \in H^3\big([0,t_{\mathrm{f}}]\big)$ satisfy $f_x(0,t) = f_x(L,t) = 0$ for all $t \in (0,t_{\mathrm{f}})$, $\eta'(0) = \eta'(1) = 0$ and $h(t) \neq 0$ for all $t \in [0,t_{\mathrm{f}}]$. We also assume that $k(0)$ is given and known. Then the inverse problem (15)–(18) can have at most one solution $\big(z(x,t), k(t)\big) \in \mathcal{W} := \Big\{z \in \mathcal{V}, z_x \in \mathcal{V}, z_{xx} \in \mathcal{V}, 0 \leq k \in L^\infty\big([0,t_{\mathrm{f}}]\big)\Big\}$, where $\mathcal{V} := \big\{v \in H^2(Q), v_{xxt} \in L^2(Q)\big\}$.*

Proof. Assume that the inverse problem has two solutions $\big(z_i(x,t), k_i(t)\big) \in \mathcal{W}$ for $i = 1, 2$, and denote $Z := z_1 - z_2$ and $K := k_1 - k_2$. Then

$$Z_{tt} - Z_{xx} + \big(1 + k_1(t)\big)Z_t + z_{2t}K(t) + \big(k_1(t) + k_1'(t)\big)Z + z_2\big(K(t) + K'(t)\big) = 0, \quad (x,t) \in Q. \tag{19}$$

Applying this equation at $x = 0$ and imposing (17) we obtain

$$-Z_{xx}(0,t) + h'(t)K(t) + h(t)\big(K(t) + K'(t)\big) = 0, \quad t \in (0, t_{\mathrm{f}}). \tag{20}$$

Using that $K(0) = 0$ and integrating (20) result in

$$K(t) = \frac{\int_0^t e^{\xi - t} Z_{xx}(0,\xi) d\xi}{h(t)}, \quad t \in [0, t_{\mathrm{f}}). \tag{21}$$

Differentiating (21) results in

$$K(t) + K'(t) = \frac{Z_{xx}(0,t)h(t) - \Big(\int_0^t e^{\xi - t} Z_{xx}(0,\xi) d\xi\Big) h'(t)}{h^2(t)}, \quad t \in [0, t_{\mathrm{f}}). \tag{22}$$

Plugging back (21) and (22) into (19) results in the following hyperbolic PDE, which is independent of the unknown blood perfusion coefficient $k(t)$:

$$\begin{aligned} &Z_{tt} - Z_{xx} + \big(1 + k_1(t)\big) Z_t + \big(k_1(t) + k_1'(t)\big) Z + z_{2t} \cdot \frac{\int_0^t e^{\xi - t} Z_{xx}(0,\xi) d\xi}{h(t)} \\ &+ z_2 \cdot \left(\frac{Z_{xx}(0,t)h(t) - \Big(\int_0^t e^{\xi - t} Z_{xx}(0,\xi) d\xi\Big) h'(t)}{h^2(t)} \right) = 0, \quad (x,t) \in Q. \end{aligned} \tag{23}$$

We also have that

$$Z(x,0) = Z_t(x,0) = 0, \quad x \in (0, L), \tag{24}$$

$$Z_x(0,t) = Z_x(L,t) = 0, \; Z(0,t) = 0, \quad t \in [0, t_{\mathrm{f}}). \tag{25}$$

Differentiating (23) with respect to x and substituting $x = 0$ and then $x = L$, we obtain that $Z_{xxx}(0,t) = Z_{xxx}(L,t) = 0$ for $t \in [0, t_{\mathrm{f}})$. Differentiating again with respect to x and setting $\nu := Z_{xx}$ we get

$$\begin{aligned} &\nu_{tt} - \nu_{xx} + \big(1 + k_1(t)\big) \nu_t + \big(k_1(t) + k_1'(t)\big) \nu = -z_{2txx} \cdot \frac{\int_0^t e^{\xi - t} Z_{xx}(0,\xi) d\xi}{h(t)} \\ &- z_{2xx} \cdot \left(\frac{Z_{xx}(0,t)h(t) - \Big(\int_0^t e^{\xi - t} Z_{xx}(0,\xi) d\xi\Big) h'(t)}{h^2(t)} \right) = 0, \quad (x,t) \in Q, \end{aligned} \tag{26}$$

and

$$\begin{aligned} \nu_x(0,t) = \nu_x(L,t) = 0, \quad t \in [0, t_{\mathrm{f}}), \\ \nu(x,0) = \nu_t(x,0) = 0, \quad x \in (0, L). \end{aligned}$$

Following the proof of Theorem 3 of [21], using integration by parts, Young's inequality and Gronwall's lemma one can obtain that

$$\int_0^L \big[\nu_t^2 + \nu_x^2 + \nu^2 + \nu_{xx}^2 + \nu_{xt}^2\big] dx \leq 0, \quad \forall t \in [0, t_{\mathrm{f}}).$$

This gives $\nu(x,t) \equiv 0$ in Q, and using the zero initial and boundary conditions (24) and (25) on Z it follows that $Z \equiv 0$ in Q, i.e. $z := z_1 \equiv z_2$ in Q. Then,

$$z_{tt} - z_{xx} + \big(1 + k_i(t)\big) z_t + \big(k_i(t) + k_i'(t)\big) z = f, \quad i = 1, 2,$$

implies by subtraction that

$$K(t) z_t + \big(K(t) + K'(t)\big) z = 0.$$

Applying this at $x = 0$ and using (18) yield by integration that $K(t) = \dfrac{Ce^{-t}}{h(t)}$, where C is a constant. Now using that $K(0) = 0$ implies that $K \equiv 0$, i.e. $k_1 \equiv k_2$. This concludes the uniqueness of solution stated in the theorem.

Example. A simple example satisfying the conditions of Theorem 1 is given by the data: $\eta(x) = 1$ for $x \in (0, L)$, $h(t) = 1$ for $t \in [0, t_{\mathrm{f}}]$, $f(x,t) = t + 1$ for $(x,t) \in Q$, $k(0) = 0$, with the unique solution given by $z(x,t) = 1$ for $(x,t) \in Q$ and $k(t) = t$ for $t \in [0, t_{\mathrm{f}}]$.

Remark. Theorem 1 establishes the uniqueness of solution of the inverse problem (15)–(18). Establishing the existence of a solution may, in principle, be attempted along the lines of [21, Section 2], but this investigation is deferred to a future work.

Before we proceed with the inversion, in Section 3, we solve the linear and well-posed direct problem (15)–(17) when the non-dimensional blood perfusion coefficient $k(t)$ is considered to be known, utilizing a FDM based on the Crank–Nicolson scheme. Additionally, the convergence of the direct solver is confirmed using a benchmark example.

3. Numerical solution of direct problem

Prior to addressing the inverse problem (15)–(18), we explore the numerical solution of the direct problem (15)–(17), assuming that the blood perfusion coefficient $k(t)$ is known.

To facilitate this, we introduce an intermediate variable υ, [8], as

$$\upsilon(x,t) := \frac{\partial z}{\partial t}(x,t) + (1 + k(t)) z(x,t), \quad (x,t) \in Q. \tag{27}$$

Introducing (27) in (15), we obtain

$$\frac{\partial \upsilon}{\partial t}(x,t) = \frac{\partial^2 z}{\partial x^2}(x,t) - k(t) z(x,t) + f(x,t), \quad (x,t) \in Q. \tag{28}$$

From (16) and (27), we obtain the initial condition

$$\upsilon(x,0) = (1 + k(0))\eta(x), \quad x \in (0, L). \tag{29}$$

We subdivide the solution domain $Q = (0, L) \times (0, t_{\mathrm{f}})$ into $M \times N$ subintervals of equal step lengths $\Delta x = L/M$ and $\Delta t = t_{\mathrm{f}}/N$, respectively. We denote $z_{m,n} := z(x_m, t_n)$, $\upsilon_{m,n} := \upsilon(x_m, t_n)$, $k_n := k(t_n)$ and $f_{m,n} := f(x_m, t_n)$, where $x_m = m\Delta x$ and $t_n = n\Delta t$ for

$m = \overline{0, M}$ and $n = \overline{0, N}$. Utilizing the Crank–Nicolson method, equations (27) and (28) are discretized as follows:

$$\frac{z_{m,n+1} - z_{m,n}}{\Delta t} = \frac{1}{2}\big(\upsilon_{m,n} - (1 + k_n)z_{m,n} + \upsilon_{m,n+1} - (1 + k_{n+1})z_{m,n+1}\big),$$
$$m = \overline{0, M}, \quad n = \overline{0, (N-1)}, \tag{30}$$
$$\frac{\upsilon_{m,n+1} - \upsilon_{m,n}}{\Delta t} = \frac{1}{2}\left(\frac{1}{(\Delta x)^2}\delta_x^2 z_{m,n} - k_n z_{m,n} + f_{m,n} + \frac{1}{(\Delta x)^2}\delta_x^2 z_{m,n+1} - k_{n+1} z_{m,n+1} + f_{m,n+1}\right),$$
$$m = \overline{0, M}, \quad n = \overline{0, (N-1)}, \tag{31}$$

where $z_{-1,n} = z(-\Delta x, t_n)$ and $z_{M+1,n} = z(L + \Delta x, t_n)$ for $n = \overline{0, N}$, and $\delta_x^2 z_{m,n} := z_{m-1,n} - 2z_{m,n} + z_{m+1,n}$. Equations (16) and (29) are discretized as

$$z_{m,0} = \eta(x_m), \quad \upsilon_{m,0} = (1 + k(0))\eta(x_m), \quad m = \overline{0, M}, \tag{32}$$

and equation (17) is discretized as

$$\frac{z_{1,n} - z_{-1,n}}{2(\Delta x)} = 0, \quad \frac{z_{M+1,n} - z_{M-1,n}}{2(\Delta x)} = 0, \quad n = \overline{0, N}. \tag{33}$$

Solving (30) for $\upsilon_{m,n+1}$, we yield

$$\upsilon_{m,n+1} = \left(1 + k_{n+1} + \frac{2}{\Delta t}\right)z_{m,n+1} + \left(1 + k_n - \frac{2}{\Delta t}\right)z_{m,n} - \upsilon_{m,n}, \tag{34}$$

for $m = \overline{0, M}$, $n = \overline{0, (N-1)}$. Introducing (34) in (31), we yield

$$-Az_{m-1,n+1} + B_{n+1}z_{m,n+1} - Az_{m+1,n+1} = Az_{m-1,n} + C_n z_{m,n} + Az_{m+1,n} + 2\upsilon_{m,n} + \frac{\Delta t}{2}\big(f_{m,n} + f_{m,n+1}\big), \tag{35}$$

for $m = \overline{0, M}$, $n = \overline{0, (N-1)}$, where $A := \dfrac{\Delta t}{2(\Delta x)^2}$, $B_n := \dfrac{2}{\Delta t} + \dfrac{\Delta t}{(\Delta x)^2} + 1 + \left(1 + \dfrac{\Delta t}{2}\right)k_n$ and $C_n := \dfrac{2}{\Delta t} - \dfrac{\Delta t}{(\Delta x)^2} - 1 - \left(1 + \dfrac{\Delta t}{2}\right)k_n$ for $n = \overline{0, N}$.

At every time step $t_{n+1} = (n+1)\Delta t$ for $n = \overline{0, (N-1)}$, using the conditions given in (33), we can recast equations (34) and (35) as:

$$\tilde{A}\boldsymbol{z}_{n+1} = \tilde{B}\boldsymbol{z}_n + 2\boldsymbol{\upsilon}_n + \boldsymbol{r}, \tag{36}$$
$$\boldsymbol{\upsilon}_{n+1} = \left(1 + k_{n+1} + \frac{2}{\Delta t}\right)\boldsymbol{z}_{n+1} + \left(1 + k_n - \frac{2}{\Delta t}\right)\boldsymbol{z}_n - \boldsymbol{\upsilon}_n, \tag{37}$$

where:

$$\boldsymbol{z}_n = \big(z_{0,n}, \ldots, z_{M,n}\big)^{\mathrm{T}}, \quad \boldsymbol{\upsilon}_n = \big(\upsilon_{0,n}, \ldots, \upsilon_{M,n}\big)^{\mathrm{T}},$$

$$\tilde{A} = \begin{pmatrix} B_{n+1} & -2A & 0 & 0 & 0 & \dots & 0 & 0 \\ -A & B_{n+1} & -A & 0 & 0 & \dots & 0 & 0 \\ 0 & -A & B_{n+1} & -A & 0 & \dots & 0 & 0 \\ 0 & 0 & -A & B_{n+1} & -A & \dots & 0 & 0 \\ \vdots & \vdots & \vdots & \ddots & \ddots & \ddots & \vdots & \vdots \\ 0 & 0 & 0 & \dots & -A & B_{n+1} & -A & 0 \\ 0 & 0 & 0 & \dots & 0 & -A & B_{n+1} & -A \\ 0 & 0 & 0 & \dots & 0 & 0 & -2A & B_{n+1} \end{pmatrix},$$

$$\tilde{B} = \begin{pmatrix} C_n & 2A & 0 & 0 & 0 & \dots & 0 & 0 \\ A & C_n & A & 0 & 0 & \dots & 0 & 0 \\ 0 & A & C_n & A & 0 & \dots & 0 & 0 \\ 0 & 0 & A & C_n & A & \dots & 0 & 0 \\ \vdots & \vdots & \vdots & \ddots & \ddots & \ddots & \vdots & \vdots \\ 0 & 0 & 0 & \dots & A & C_n & A & 0 \\ 0 & 0 & 0 & \dots & 0 & A & C_n & A \\ 0 & 0 & 0 & \dots & 0 & 0 & 2A & C_n \end{pmatrix}, \quad \boldsymbol{r} = \begin{pmatrix} \frac{\Delta t}{2}\big(f_{0,n} + f_{0,n+1}\big) \\ \frac{\Delta t}{2}\big(f_{1,n} + f_{1,n+1}\big) \\ \vdots \\ \frac{\Delta t}{2}\big(f_{M-1,n} + f_{M-1,n+1}\big) \\ \frac{\Delta t}{2}\big(f_{M,n} + f_{M,n+1}\big) \end{pmatrix}.$$

We proceed to examine a numerical illustration to validate the convergence and accuracy of the proposed FDM scheme.

3.1 Verification example

We examine the direct problem (15)–(17) with $L = t_{\mathrm{f}} = 1$ and the input data:

$$z(x,0) = \eta(x) = \cos(\pi x), \quad \frac{\partial z}{\partial t}(x,0) = 0, \tag{38}$$

$$f(x,t) = 2 + 2t(1+t) + \pi^2 \cos(\pi x) + (t+1)(t^2 + \cos(\pi x)), \tag{39}$$

and

$$k(t) = t. \tag{40}$$

Subsequently, the exact solution is expressed as

$$z(x,t) = t^2 + \cos(\pi x). \tag{41}$$

The root mean square error (RMSE) given by

$$\mathrm{RMSE}(h) = \left[\frac{1}{N+1} \sum_{n=0}^{N} \Big(h^{\mathrm{numerical}}(t_n) - h^{\mathrm{exact}}(t_n) \Big)^2 \right]^{1/2} \tag{42}$$

was attained as $\mathrm{RMSE}(h) \in \{0.0317, 0.0079, 0.002\}$ for $M = N \in \{5, 10, 20\}$, respectively. This indicates second-order convergence of the FDM.

4. Numerical approach to solve the inverse problem

To accurately and stably reconstruct the time-dependent blood perfusion coefficient $k(t)$

along with the temperature $z(x,t)$ satisfying (15)–(18), we minimize the cost function given by

$$G(k) = \|z(0,t) - h(t)\|^2 + \gamma \|k(t)\|^2, \tag{43}$$

where z solves the direct problem (15)–(17) for given $k(t)$, $\gamma \geq 0$ is a regularization parameter and the norm is the L^2-norm. The discretized form of (43) is

$$G(\boldsymbol{k}) = \sum_{n=1}^{N} \big[z(0,t_n) - h(t_n)\big]^2 + \gamma \sum_{n=1}^{N} k_n^2. \tag{44}$$

The subroutine *lsqnonlin* from the MATLAB optimization toolbox is employed to minimize the cost function (44) subject to the simple bounds $0 \leq k \leq \mathcal{M}$, where $\mathcal{M}$ is a large number.

The resolution of the inverse problem (15)–(18) is conducted under both noise-free and perturbed boundary measurements The perturbed boundary measurement is numerically simulated as:

$$h^{\epsilon}(t_n) = h(t_n) + \epsilon_n, \quad n = \overline{1,N}, \tag{45}$$

where ϵ_n are random variables generated from a Gaussian normal distribution with zero mean and standard deviation

$$\sigma = p \times \max_{t \in [0,t_{\mathrm{f}}]} |h(t)|, \tag{46}$$

where p denotes the percentage of noise. The random variables $\boldsymbol{\epsilon} = (\epsilon_n)_{n=\overline{1,N}}$ are generated using the MATLAB function $normrnd(0,\sigma,N)$. In the case of perturbed boundary measurement (45), $h(t_n)$ in (44) is substituted with $h^{\epsilon}(t_n)$.

5. Numerical results and discussion

We herein carry out numerical tests to verify the inversion algorithm's convergence, stability and accuracy. To measure the numerical solutions' accuracy, the root mean square error (RMSE) given by

$$\mathrm{RMSE}(k) = \left[\frac{t_{\mathrm{f}}}{N} \sum_{n=1}^{N} \Big(k^{\mathrm{numerical}}(t_n) - k^{\mathrm{exact}}(t_n) \Big)^2 \right]^{1/2} \tag{47}$$

is used. We set $t_{\mathrm{f}} = 1$, for simplicity. The lower and upper bounds for the unknown blood perfusion coefficient $k(t)$ are set as 0 and 10^2, respectively.

We consider the inverse problem (15)–(18) with an unknown blood perfusion coefficient and the input data (38) and (39). As for the extra boundary measurement (18), we consider

$$h(t) = z(0,t) = t^2 + 1. \tag{48}$$

It can be readily observed that the input data mentioned above satisfy the conditions of Theorem 1. Consequently, the uniqueness of the solution is assured. It can be verified through direct substitution that the exact solution is given by (41) for $z(x,t)$ and (40) for $k(t)$. We take the initial guess:

$$k^0(t_n) = k(0) = 0, \quad n = \overline{1,N}. \tag{49}$$

We set $M = N = 40$ and begin the process of finding the time-dependent blood perfusion coefficient $k(t)$ in the absence of noise in the data $h(t)$, i.e. with $p = 0$ in (46). The behaviour of the cost function G over the number of iterations, without employing regularization, i.e. with $\gamma = 0$, is illustrated in Figure 1(a). Notably, we observe swift and monotonic decreasing convergence towards an exceedingly small value of $\mathcal{O}(10^{-27})$ in only 9 iterations. Furthermore, in Figure 1(b), we compare the resulting reconstruction of the time-dependent blood perfusion coefficient $k(t)$ with the exact solution (40). The achieved RMSE for the function $k(t)$ is remarkably small, with a value of $\mathcal{O}(10^{-3})$. This clearly demonstrates that our approach has successfully yielded an accurate and stable solution for the time-dependent blood perfusion coefficient $k(t)$ when the data (48) is free of noise.

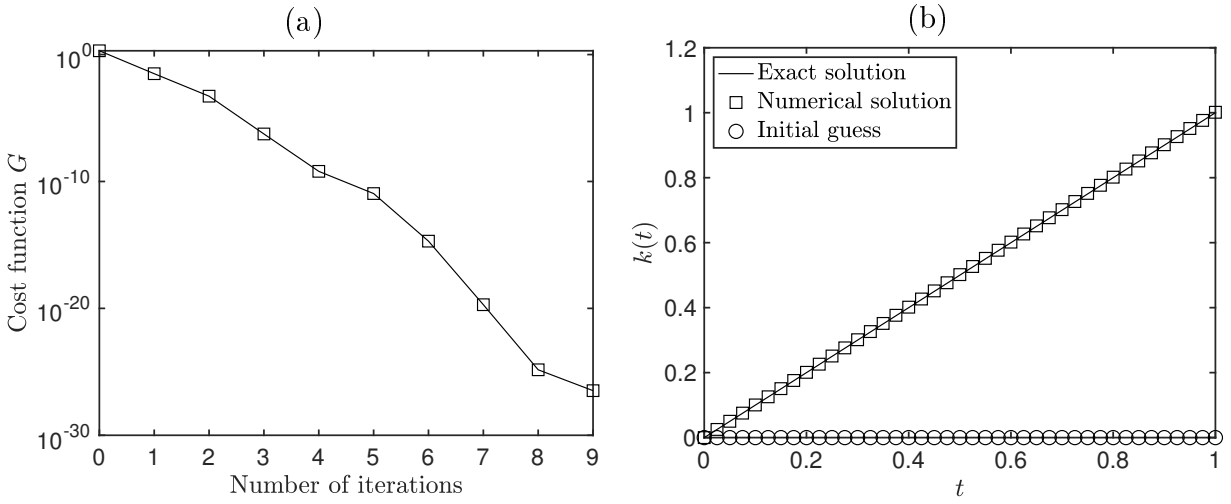

Figure 1: (a) The cost function (44) with $\gamma = 0$ and (b) the comparison of the exact (40) and numerical solutions for $k(t)$, without any noise and regularization.

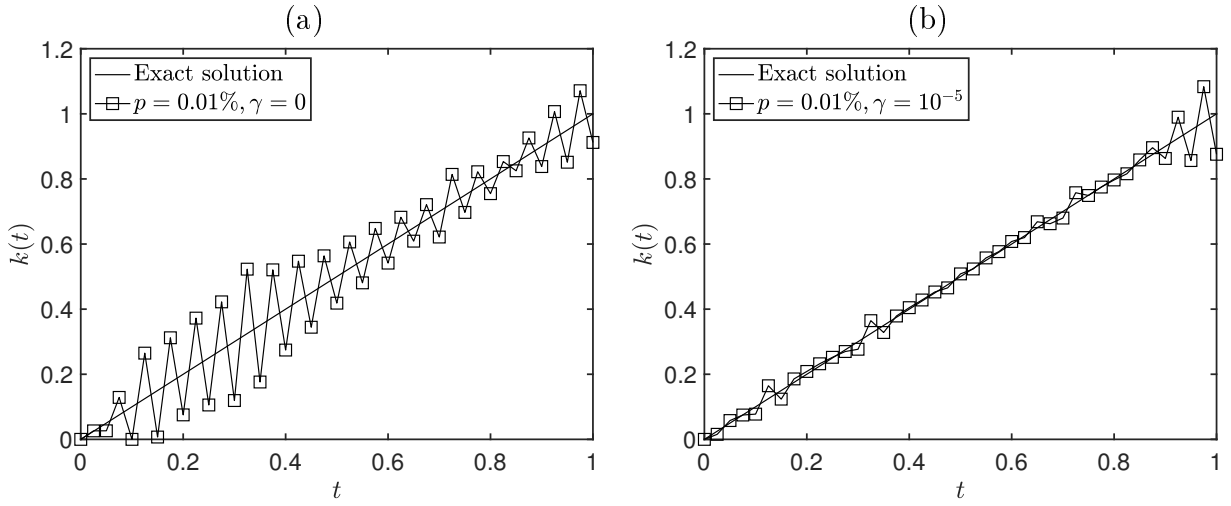

Figure 2: Comparison of the exact (40) and numerical solutions for $k(t)$, for $p = 0.01\%$ noise and (a) $\gamma = 0$ (i.e. without regularization) and (b) $\gamma = 10^{-5}$ (i.e. with regularization).

Let us investigate the stability of the numerical solution when noise is added to the boundary data (48). We include $p \in \{0.01, 0.1\}\%$ noise to the data (48) using (45) and (46). Figures 2 and 3 showcase the determined blood perfusion coefficient $k(t)$, without and with regularization. Notably, Figures 2(a) and 3(a) reveal that the reconstruction outcomes for the function $k(t)$ without regularization exhibit oscillations, resulting in $\text{RMSE}(k) \in \{0.1026, 0.3513\}$. These oscillations were anticipated due to the inherently ill-posed nature of the problem (15)–(18) and its sensitivity to minor variations in the boundary measurement (18). Hence, regularization becomes essential to restore the solution's stability. As previously mentioned, we utilize the Tikhonov regularization and fine-tune its parameter through an iterative process. Initially, a low γ is employed and incrementally increased until the high oscillations vanish. Through this process, it is determined that setting $\gamma = 10^{-5}$ for $p = 0.01\%$ noise and $\gamma = 10^{-3}$ for $p = 0.1\%$ noise ensures accuracy and stability in the numerical outcomes for the function $k(t)$. Consequently, this leads to significantly reduced $\text{RMSE}(k) = 0.0354$ for $p = 0.01\%$ noise and $\text{RMSE}(k) = 0.0876$ for $p = 0.1\%$ noise, as depicted in Figures 2(b) and 3(b), respectively. Figure 4 displays the numerical solution for $z(x, t)$ along with the exact solution (41) and the absolute errors between them. Further detailed information regarding the RMSE values (47), the minimum value of (44), the number of iterations and the elapsed time, without and with regularization, can be found in Table 1. The outcomes presented in this example demonstrate that as the percentage of noise p diminishes from 0.1% to 0.01% and then to zero, the convergence of the numerical solution for the pair $\{z(x, t), k(t)\}$ is attained provided that regularization is applied.

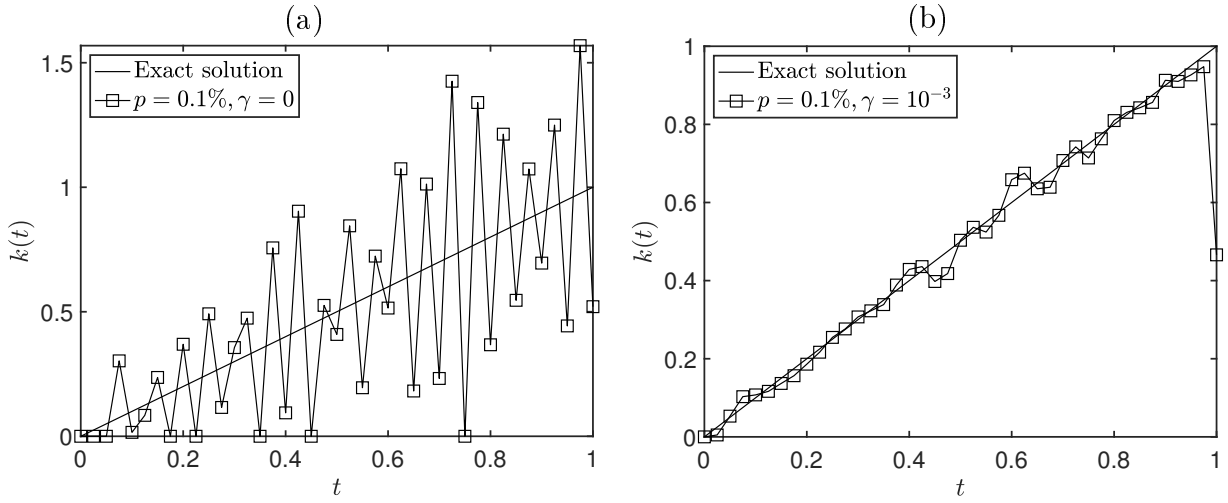

Figure 3: Comparison of the exact (40) and numerical solutions for $k(t)$, for $p = 0.1\%$ noise and (a) $\gamma = 0$ (i.e. without regularization) and (b) $\gamma = 10^{-3}$ (i.e. with regularization).

6. Conclusions

The inverse problem of determining the time-dependent blood perfusion coefficient and the temperature in the thermal-wave model of bio-heat transfer from extra boundary temperature measurement is explored. The unique solvability of this inverse coefficient problem is established. To address this problem computationally, it is recast as a nonlinear least-squares

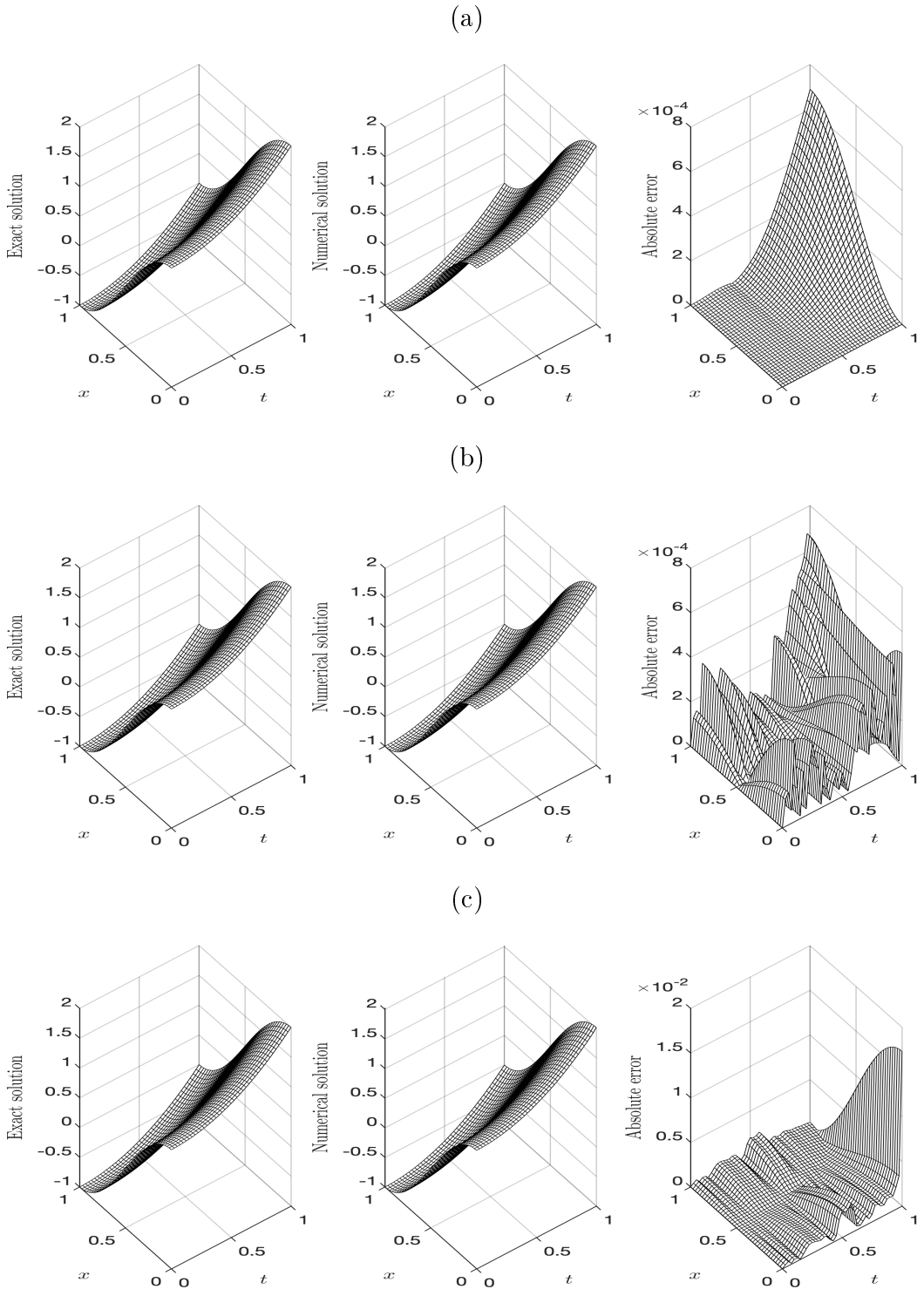

Figure 4: The exact (41) and numerical solutions for $z(x,t)$, for (a) $p = 0$ and $\gamma = 0$ (i.e. without any noise and regularization), (b) $p = 0.01\%$ noise and $\gamma = 10^{-5}$, and (c) $p = 0.1\%$ noise and $\gamma = 10^{-3}$. The absolute errors are also included.

Table 1: The RMSE values (47), the minimum value of (44), the number of iterations and the elapsed time, for $p \in \{0, 0.01\%, 0.1\%\}$ noise, without and with regularization.

p	γ	RMSE(k)	Minimum value of (44)	Iter	Time
0	0	1.4×10^{-3}	3.3×10^{-27}	9	2 s
0.01%	0	0.1026	1.05×10^{-8}	25	3 s
	10^{-7}	0.0835	1.43×10^{-6}	52	6 s
	10^{-6}	0.0444	1.40×10^{-5}	40	5 s
	10^{-5}	0.0354	1.39×10^{-4}	44	4 s
	10^{-4}	0.0505	1.37×10^{-3}	39	4 s
0.1%	0	0.3513	1.65×10^{-5}	54	8 s
	10^{-5}	0.1460	1.70×10^{-4}	50	9 s
	10^{-4}	0.0900	1.44×10^{-3}	44	5 s
	10^{-3}	0.0876	1.34×10^{-2}	44	5 s
	10^{-2}	0.1610	1.15×10^{-1}	45	5 s

minimization problem with simple constraints on the unknown coefficient, and stability is ensured through the application of the Tikhonov regularization. The Crank–Nicolson finite-difference scheme is utilized to solve the direct problem, while the iterative resolution of the nonlinear least-squares minimization problem is conducted by the *lsqnonlin* routine from the MATLAB optimization toolbox. Numerical results for a benchmark test example are presented and thoroughly discussed, providing insights into the performance and effectiveness of the proposed methodology.

References

[1] M. Alosaimi, D. Lesnic and J. Niesen (2020) "Reconstruction of the thermal properties in a wave-type model of bio-heat transfer", *Int. J. Numer. Meth. Heat & Fluid Flow*, Vol. 30, pp. 5143-5167.

[2] M. Alosaimi, D. Lesnic and J. Niesen (2021) "Determination of the thermo-physical properties of multi-layered biological tissues", *Appl. Math. Model.*, Vol. 99, pp. 228-242.

[3] M. Alosaimi and D. Lesnic (2023) "Determination of the space-dependent blood perfusion coefficient in the thermal-wave model of bio-heat transfer", *Eng. Comput.*, Vol. 40, pp. 411-433.

[4] H. Arkin, L.X. Xu and K.R. Holmes (1994) "Recent developments in modelling heat transfer in blood perfused tissues", *IEEE Trans. Biomed. Eng.*, Vol. 41, pp. 97-107.

[5] J.R. Cannon (1963) "The solution of the heat equation subject to the specification of energy", *Quart. Appl. Math.*, Vol. 21, pp. 155-160.

[6] J.R. Cannon and J. van der Hoek (1986) "Diffusion subject to the specification of mass", *J. Math. Anal. Appl.*, Vol. 115, pp. 517-529.

[7] C.I. Christov and P.M. Jordan (2005) "Heat conduction paradox involving second-sound propagation in moving media", *Phys. Rev. Lett.*, Vol. 94, Art. 154301, (4 pages).

[8] W. Dai and R. Nassar (1999) "A finite difference scheme for solving the heat transport equation at the microscale", *Numer. Meth. Partial Diff. Eqns.*, Vol. 15, pp. 697-708.

[9] W. Dai, H. Wang, P.M. Jordan, R.E. Mickens, and A. Bejan (2008) "A mathematical model for skin burn injury induced by radiation heating", *Int. J. Heat Mass Transfer*, Vol. 51, pp. 5497-5510.

[10] Y.-L. Fang, D. Lesnic and M. Alosaimi (2023) "Inverse problems of damped wave equations with Robin boundary conditions: an application to blood perfusion", *Inverse Problems*, Vol. 39, Art. 065008, (32 pages).

[11] A. Hasanov Hasanoglu and V.G. Romanov (2021) "Introduction to Inverse Problems for Differential Equations", 2nd edn., Springer, Berlin.

[12] V. Isakov (2017) "Inverse Problems for Partial Differential Equations", 3rd edn., Springer, Berlin.

[13] A. Jalali, M.B. Ayani, and M. Baghban (2014) "Simultaneous estimation of controllable parameters in a living tissue during thermal therapy", *J. Thermal Biology*, Vol. 45, pp. 37-42.

[14] E. Kengne and A. Lakhssassi (2015) "Bioheat transfer problem for one-dimensional spherical biological tissues", *Math. Biosciences*, Vol. 269, pp. 1-9.

[15] D. Lesnic (2021) "Inverse Problems with Applications in Science and Engineering", CRC Press, Taylor & Francis Group, Abingdon, UK.

[16] K. Mitra, S. Kumar, A. Vedevarz, and M.K. Moallemi (1995) "Experimental evidence of hyperbolic heat conduction in processed meat", *J. Heat Transfer*, Vol. 117, pp. 568-573.

[17] H.H. Pennes (1948) "Analysis of tissue and arterial blood temperatures in the resting human forearm", *J. Appl. Physiology*, Vol. 1, pp. 93-122.

[18] A.I. Prilepko, D.G. Orlovsky and I.A. Vasin (2000) "Methods for Solving Inverse Problems in Mathematical Physics", CRC Press, Boca Raton, Florida.

[19] M. Ragab, A.E. Abouelregal, H.F. AlShaibi and R.A. Mansouri (2021) "Heat transfer in biological spherical tissues during hyperthermia of magnetoma", *Biology*, Vol. 10, Art. 1259, (16 pages).

[20] Z.P. Ren, J. Liu, C.C. Wang, and P.X. Jiang (1995) "Boundary element method (BEM) for solving normal or inverse bio-heat transfer problem of biological bodies with complex shape", *J. Thermal Sci.*, Vol. 4, pp. 117-124.

[21] R.R. Safiullova (2018) "Solvability of nonlinear inverse problem for hyperbolic equation", *J. Math. Sci.*, Vol. 228, pp. 431-448.

[22] P. Wainwright (2000) "Thermal effects of radiation from cellular telephones", *Phys. Med. Biol.*, Vol. 45, pp. 2363-2372.